Vapor-Fed Electrolysis of Water Using Earth-Abundant Catalysts in Nafion or in Bipolar Nafion/ Poly(benzimidazolium) Membranes: Supporting Information

Authors: Patrick K. Giesbrecht;[1,2] Astrid M. Müller;[3,4] Carlos G. Read;[5] Steven Holdcroft;[6] Nathan S. Lewis;[5] Michael S. Freund[1,2]

Affiliations: [1]Department of Chemistry, Florida Institute of Technology, Melbourne, Florida 32901, United States; [2]Department of Chemistry, Dalhousie University, 6274 Coburg Road, Halifax, NS B3H 4R2, Canada; [3]Beckman Institute, California Institute of Technology, 1200 E. California Boulevard, Mail Code 139-74, Pasadena, California 91125, United States; [4]Department of Chemical Engineering, University of Rochester, Rochester, New York 14627, United States; [5]Division of Chemistry and Chemical Engineering, California Institute of Technology, Pasadena, California 91125, United States; [6]Department of Chemistry, Simon Fraser University, Burnaby, BC V5A 1S6, Canada

Table of Contents

1. Catalyst Films and Solution-Phase HER/OER.

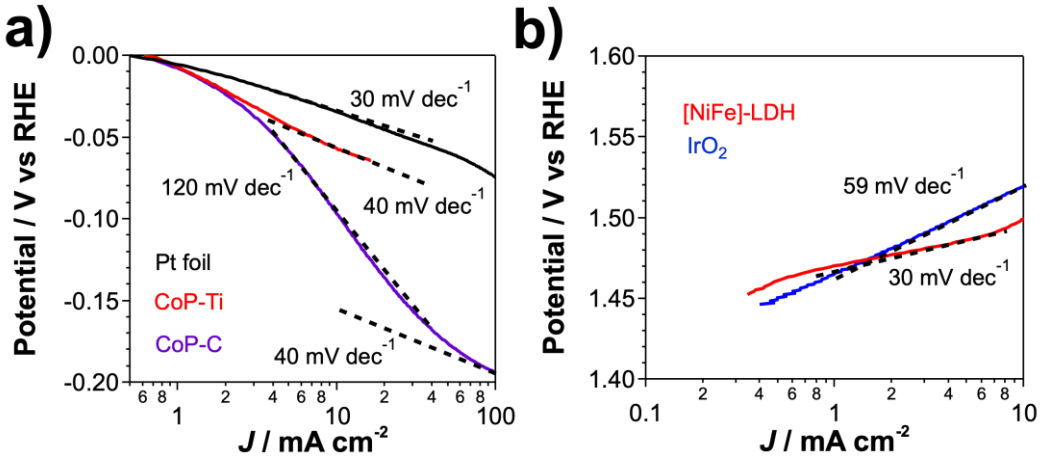

Figure S1. Tafel plots of a) HER catalyst films in 0.50 M H_2SO_4(aq); and b) OER catalyst films in 1.0 M KOH(aq). Dashed lines in a) represent predicted Tafel slopes for an HER electrocatalyst under operation (120, 40 and 30 mV dec^{-1}). Dashed lines in b) represent predicted Tafel slopes for an OER electrocatalyst under operation with n(1-α) =1, 2 (Tafel slopes of 59 and 30 mV dec^{-1}).[1,2]

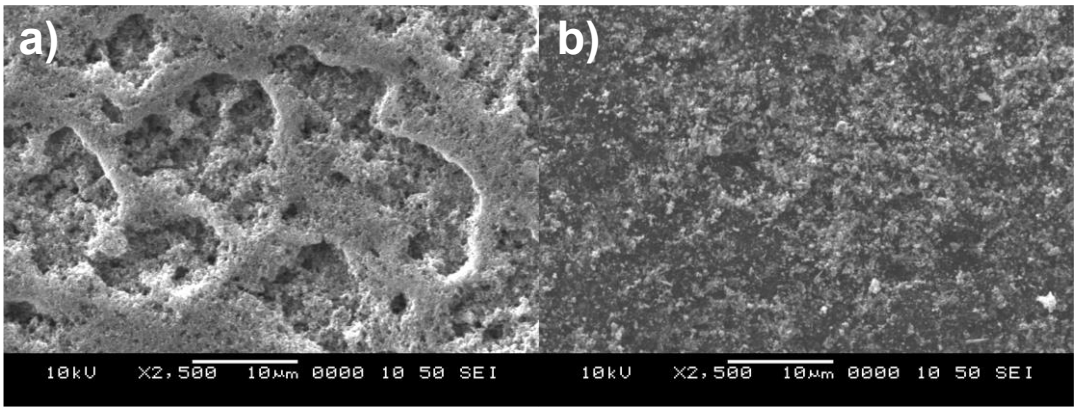

Figure S2. Scanning-electron micrographs of a) Pt/C and b) IrO_x Nafion-based films on C-paper prior to MEA incorporation. Catalyst loadings of 3 mg cm^{-2}.

Table S1. Overpotentials, Tafel slope, and exchange current densities for the cathode and anode catalysts determined in this work.

Catalyst	Loading (mg cm^{-2})	$\eta_{-10\ mA\ cm^{-2}}$ (HER, V)[a]	$\eta_{10\ mA\ cm^{-2}}$ (OER, V)[b]	Tafel Slope (mV dec^{-1})[c]	J_0 (mA cm^{-2})
Pt foil	-	-0.045	-	29	0.9
CoP-Ti[d]	2.5	-0.062	-	49	0.1
CoP-C[e]	2	-0.068	-	132; 44	-[g]
IrO_x[f]	2	-	0.300	55	$5x10^{-5}$
[NiFe]-LDH[f]	0.4	-	0.286	25; 63	$2x10^{-11}$

[a]HER in 0.50 M H_2SO_4(aq). [b]OER in 1.0 M KOH(aq). [c]Tafel slope reported at low and high overpotentials if potential-dependent. [d]CoP deposited on Ti paper. [e]CoP deposited on C-paper. [f]Dropcast film on glassy-carbon-disk electrode. [g]Potential-dependent Tafel slope prevented accurate determination of the exchange current density.

2. TP-WS Capabilities of MEAs in this work.

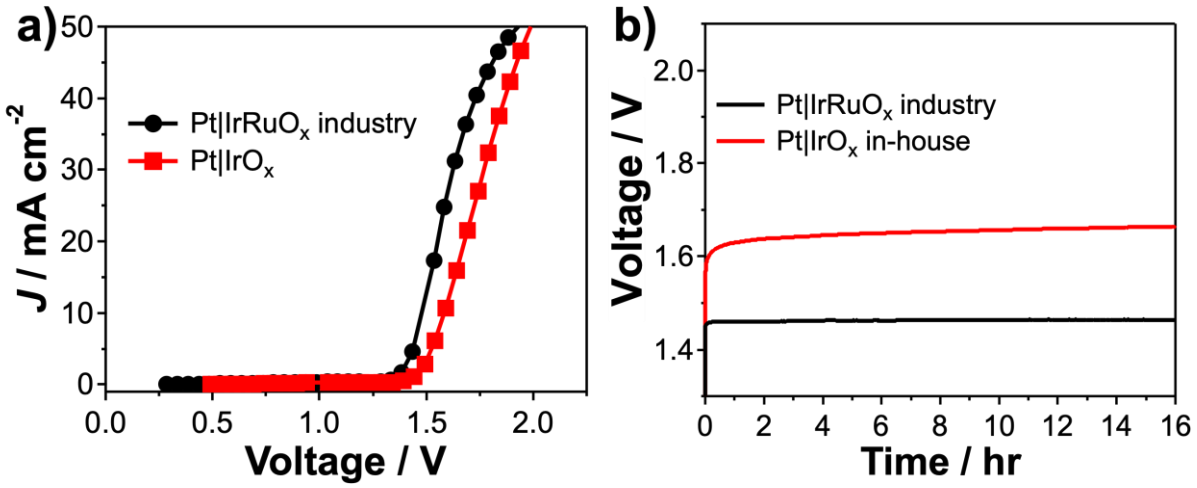

Figure S3. Comparison of the TP-WS performance in a two-electrode configuration under humid-N_2(g) flow at room temperature of a commercially available Pt|$IrRuO_x$ sample (black trace) with that of an in-house Pt|IrO_x MEA used in this work (red trace). a) Steady-state polarization data and b) constant-current electrolysis at 10 mA cm^{-2}. Catalyst loadings were 3 mg cm^{-2}.

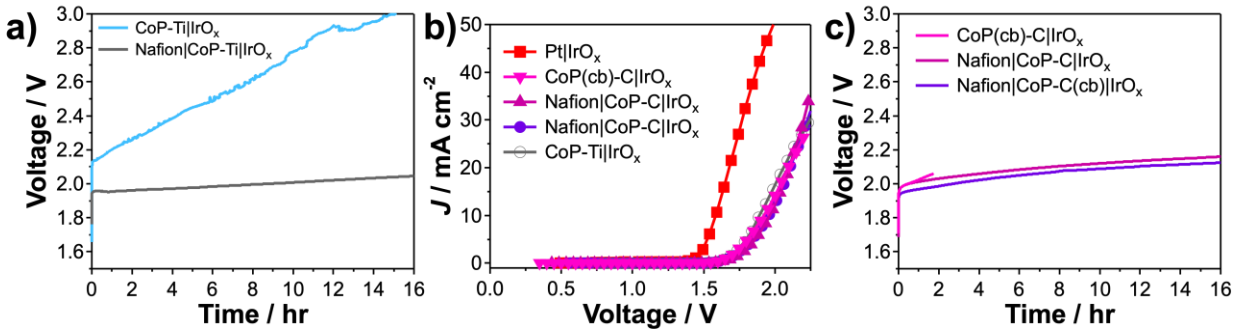

Figure S4. a) Constant-current electrolysis (10 mA cm^{-2}) data for CoP-Ti|IrO_x MEAs performing TP-WS under humid-N_2(g) flow at room temperature in the absence (blue trace) and presence (grey trace) of a Nafion overcoat. b) Steady-state polarization and c) constant-current electrolysis (10 mA cm^{-2}) data for CoP-C|IrO_x MEAs performing TP-WS under humid-N_2(g) flow at room temperature with and without C black (cb) incorporated into the CoP side or a Nafion overcoat. Nafion-based Pt/C|IrO_x MEA (red squares) shown for comparison. CoP loading of 2 mg cm^{-2} for C-paper-based cathodes. IrO_x loading of 3 mg cm^{-2} on C-paper for the anode.

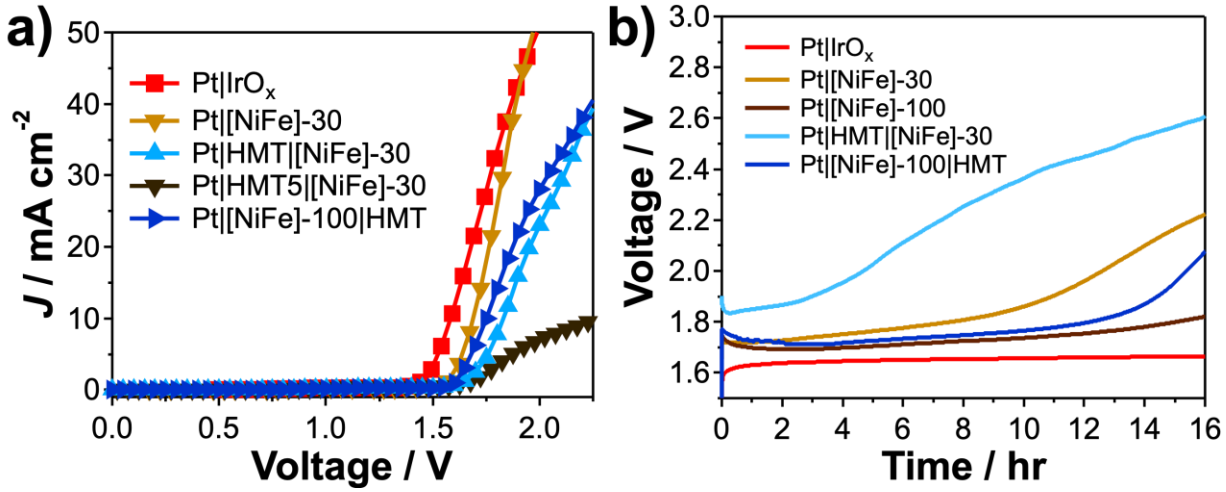

Figure S5. a) Steady-state polarization and b) constant-current electrolysis (10 mA cm^{-2}) data for [NiFe]-LDH samples performing TP-WS under humid-N_2(g) flow at room temperature with a HMT-PMBI overlayer (light blue, brown traces) and a HMT-PMBI backlayer (dark blue trace). A Nafion-based Pt/C|IrO_x MEA (red) is shown for comparison. [NiFe]-LDH loading of 0.6 mg cm^{-2} on the anode; Pt/C loading of 3 mg cm^{-2} on C-paper for the cathode.

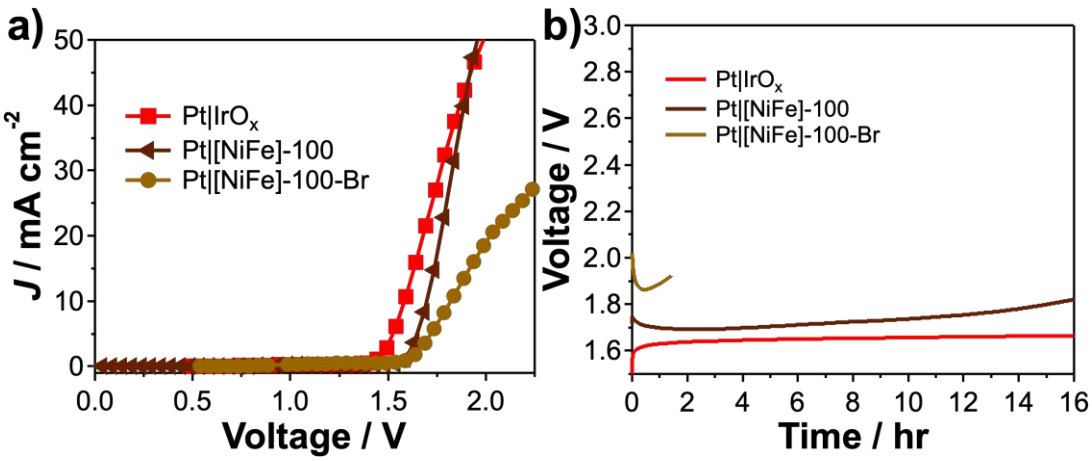

Figure S6. a) Steady-state polarization and b) constant-current electrolysis (10 mA cm^{-2}) data for [NiFe]-LDH samples performing TP-WS under humid-N_2(g) flow at room temperature with HMT-PMBI-Br (gold) or HMT-PMBI-OH (brown) as the ionomer binder. Nafion-based Pt/C|IrO_x MEA (red) shown for comparison. [NiFe]-LDH loading of 0.6 mg cm^{-2} on the anode; Pt/C loading of 3 mg cm^{-2} on C-paper for the cathode.

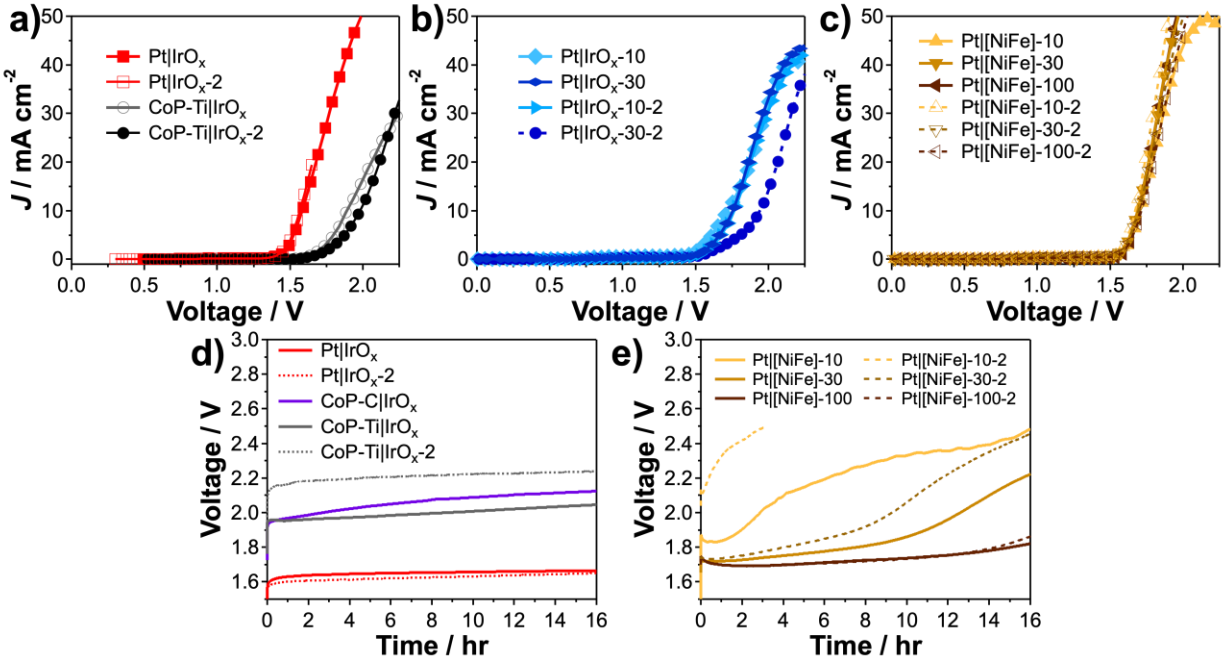

Figure S7. a-c) Steady-state polarization and d-e) constant-current electrolysis (10 mA cm^{-2}) data for multiple samples of a,d) Nafion-based Pt|IrO_x and CoP-Ti|IrO_x MEAs, b) Pt|IrO_x BPM-based MEAs, c,e) Pt|[NiFe] BPM-based MEAs performing TP-WS under humid-N_2(g) flow at room temperature. CoP loading of 2.5 mg cm^{-2} on Ti-paper or C-paper for the cathode; IrO_x loading of 3 mg cm^{-2} on C-paper for the anode; [NiFe]-LDH loading of 0.6 mg cm^{-2} on C-paper for the anode; Pt/C loading of 3 mg cm^{-2} on C-paper for the cathode.

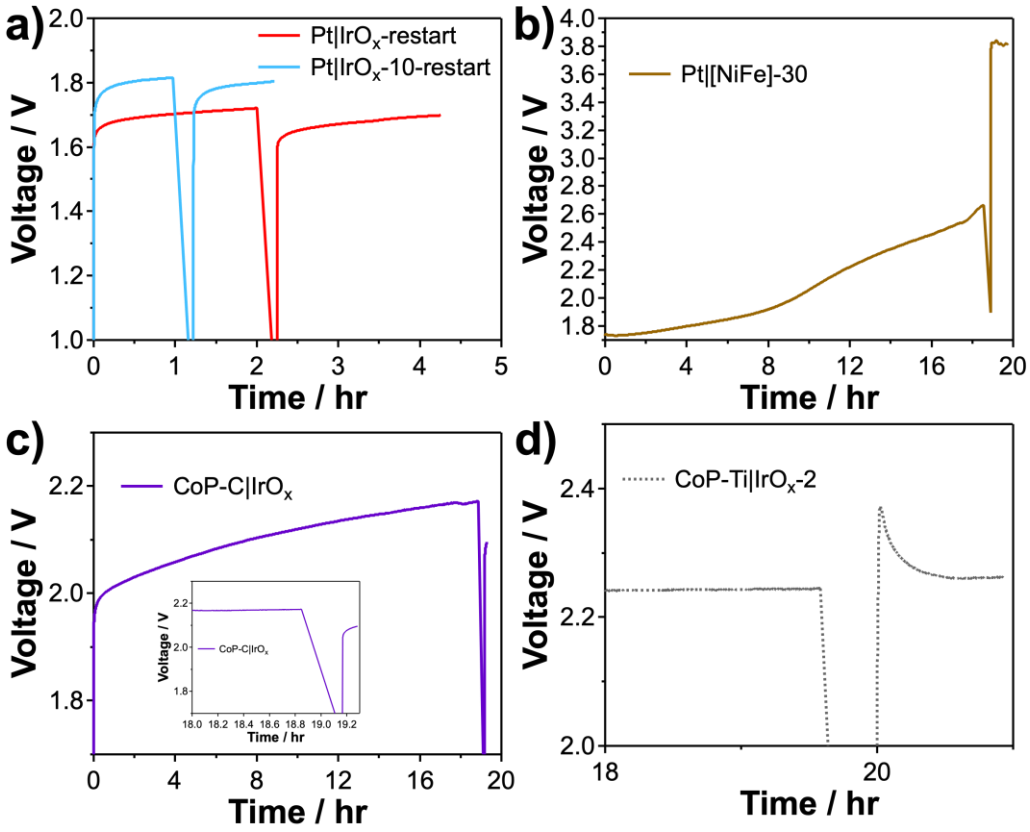

Figure S8. Constant-current electrolysis (10 mA cm^{-2}) data for a) Nafion-based (red) and BPM-based (blue) Pt|IrO_x MEAs; b) Pt|[NiFe] BPM-based MEA; c) CoP-C|IrO_x Nafion-based MEA; and d) CoP-Ti|IrO_x Nafion-based MEA before and after rehydration of the MEA under open-circuit voltage conditions. CoP loading of 2.5 mg cm^{-2} on Ti-paper or C-paper for the cathode; IrO_x loading of 3 mg cm^{-2} on C-paper for the anode; [NiFe]-LDH loading of 0.6 mg cm^{-2} on C-paper for the anode; Pt/C loading of 3 mg cm^{-2} on C-paper for the cathode.

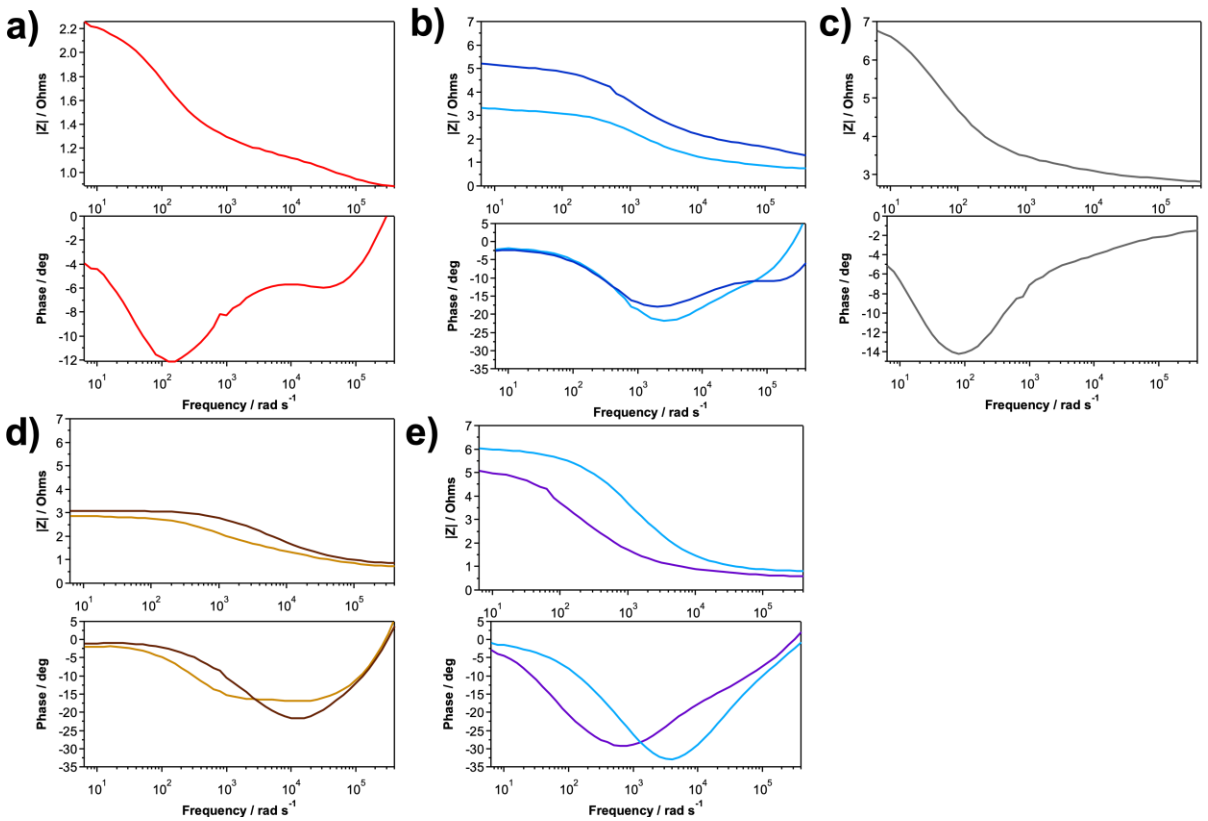

Figure S9. Bode Plots for representative MEAs at the operating voltage $V_{10\ mA\ cm^{-2}}$ for TP-WS in this work: a) Pt|IrO_x Nafion-based MEA; b) Pt|IrO_x BPM-based MEAs (Pt|IrO_x-10 light blue; Pt|IrO_x-30 dark blue); c) CoP-Ti|IrO_x MEA; d) Pt|[NiFe]-30 (gold) and Pt|[NiFe]-100 (brown) BPM-based MEAs; e) CoP-C|IrO_x MEA before (purple) and after (blue) constant-current electrolysis at 10 mA cm^{-2}.

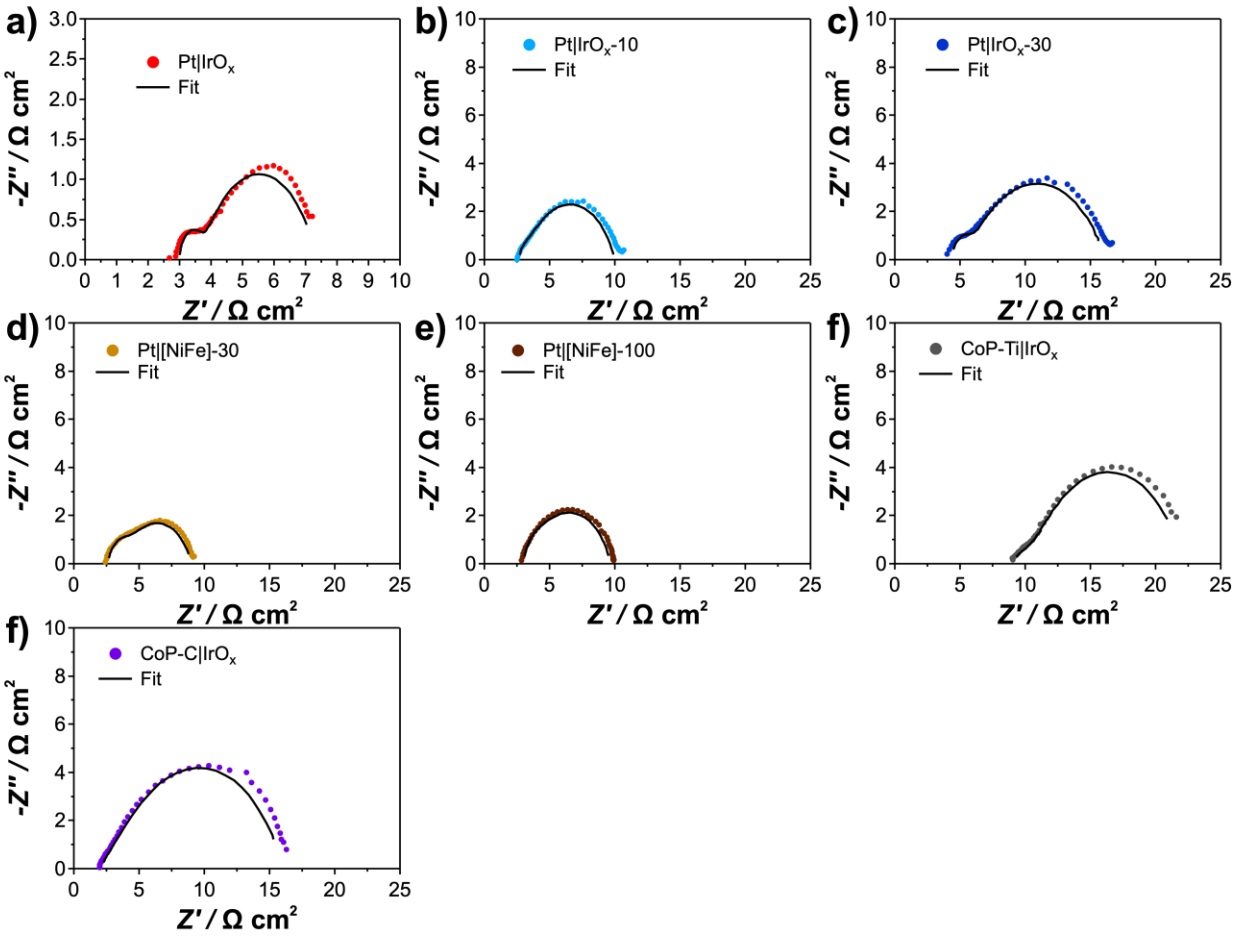

Figure S10. Equivalent circuit model fits to EIS spectra at the operating voltage $V_{10\ mA\ cm^{-2}}$ for representative MEAs in this work.

Table S2. Series, polarization, mass-transport and activation overvoltages determined from EIS data at $V_{10\ mA\ cm^{-2}}$ for representative MEAs studied in this work.

MEA	ΔV_{iR} (V)[a]	$\Delta V_{polarization}$ (V)[b]	ΔV_{mxt} (V)[c]	ΔV_{act} (V)[d]
Pt|IrO_x	0.03	0.05	0.005	0.38
Pt|IrO_x-10	0.02	0.08	0.009	0.56
Pt|IrO_x-30	0.04	0.12	0.010	0.54
CoP-Ti|IrO_x	0.09	0.13	0.012	0.60
CoP-C|IrO_x	0.02	0.14	0.010	0.75
CoP-C|IrO_x after	0.02	0.17	-	-
Pt|[NiFe]-30	0.02	0.07	0.005	0.48
Pt|[NiFe]-30 after	0.02	0.32	-	-
Pt|[NiFe]-100	0.02	0.08	0.005	0.50
Pt|[NiFe]-100 after	0.02	0.28	-	-

[a]Determined from the Z' high-frequency intercept in Nyquist plot of the EIS spectra of the MEA at $V_{10\ mA\ cm^{-2}}$. [b]Width of the Nyquist plot of the EIS spectra of the MEA at $V_{10\ mA\ cm^{-2}}$. [c]Determined

from application of Equation S1 to steady-state polarization data. [d]Determined from Equation 1 in the manuscript.

Table S3. Values of the operating voltage $V_{10\ mA\ cm^{-2}}$ and the drift in the operating voltage during constant-current electrolysis at 10 mA cm^{-2} for individual MEAs studied in this work.

MEA	$V_{10\ mA\ cm^{-2}}$ (V)[a]	ΔV_{drift} (V)[b]	Rate (mV hr^{-1})
Pt|$IrRuO_x$	1.45	0	0
Pt|IrO_x	1.60	0.05	2.8
Pt|IrO_x-2	1.59	0.05	2.8
Pt|IrO_x-10	1.72	0.06	3.3
Pt|IrO_x-30	1.75	0.03	1.7
CoP-Ti|IrO_x	1.90	0.10	5.5
CoP-Ti|IrO_x-2	2.01	0.09	5.0
CoP-C|IrO_x	1.95	0.19	10.6
Pt-Ti|IrO_x	1.70	0.19	10.6
Pt|[NiFe]-10	1.72	0.78	43.3
Pt|[NiFe]-10-2	1.74	0.76	190
Pt|[NiFe]-30	1.71	0.50	27.8
Pt|[NiFe]-30-2	1.75	0.70	38.9
Pt|[NiFe]-100	1.70	0.15	8.3
Pt|[NiFe]-100-2	1.70	0.17	9.4
Pt|HMT|[NiFe]-30	1.83	0.76	42.2
Pt|[NiFe]-100|HMT	1.75	0.32	17.8

[a]Operating voltage at 10 mA cm^{-2} as determined from steady-state polarization data. [b]Drift in $V_{10\ mA\ cm^{-2}}$ during constant-current electrolysis at 10 mA cm^{-2}.

Table S4. EIS equivalent circuit model values for representative MEAs in this work. Uncorrected for surface area of MEA.

MEA	R_s (Ω)	R_{cath} (Ω)	Q_{cath}[a]	ϕ_{cath}	R_{an} (Ω)	Q_{an}[a]	ϕ_{an}
Pt|IrO_x	0.8944	0.23592	0.0004818	0.88111	1.222	0.03866601	0.66835
Pt|IrO_x-10*	0.81403	0.23592	0.0004818	0.88111	2.212	0.0002194	0.75934
Pt|IrO_x-30	1.286	0.44631	2.4302E-05	0.98216	3.482	0.00245811	0.6883
CoP-Ti	2.741	3.528	0.01490799	0.76528	0.84837	0.02601	0.45651
CoP-C initial	0.57244	3.831	0.00631101	0.75567	0.82432	0.02221401	0.52097
CoP-C after**	0.79924	4.463	0.00140571	0.74212	0.82432	0.02221401	0.52097
Pt|[NiFe]-30	0.77181	0.4936	0.0002114	0.90747	1.635	0.00380631	0.7388
Pt|[NiFe]100	0.89998	0.28377	0.00013037	0.99547	1.936	0.00092538	0.77069

[a]Q unit is Ω^{-1} s^{ϕ}.

*Values of R_{cath}, Q_{cath}, and ϕ_{cath} were fixed to values obtained from Pt|IrO_x.

**Values of R_{an}, Q_{an}, and ϕ_{an} were kept fixed to values obtained from CoP-C initial.

Determination of the mass-transport overvoltage at 10 mA cm^{-2}.

The overvoltage associated with mass transport for TP-WS under flow can be determined by

$$\Delta V_{mxt} = \frac{RT}{nF}\left(1 + \frac{1}{\alpha}\right)\ln\left(\frac{J_{\lim}}{J_{\lim} - J}\right) \quad (S1)$$

Where R is the ideal gas constant, T temperature, n = 2, F Faraday's constant, charge-transfer coefficient α = 0.5, $J_{\lim}$ the limiting current density determined from steady-state polarization data, and J the current density of interest (10 mA cm^{-2}).

Determination of the longevity of co-ion current at 10 mA cm^{-2} in BPM-based MEAs.

$A_{geometric}$ = 3 cm^2; L_{nafion} = 0.0183 cm; L_{cath} = 0.001 cm; L_{anode} = $L_{HMT\text{-}PMBI}$ = 0.001 cm
$[M^+]_{Nafion}$ = 1.5 M; $[A^-]_{HMT\text{-}PMBI}$ = 1.5 M

Total co-ion current density time at 10 mA cm^{-2}:
$T_{total} = (n_M + n_A)*F/(0.03A)$
T_{total} = (3 cm^2)*(0.0015 mol/cm^3)*(0.0183 cm+0.002 cm)*(96485 C/mol)/(0.03A)
T_{total} = 290 s

Calculation of current contribution through carbonate removal.

From Ref [3]:
C_{CO2} = 5 ppm (via GC-MS, constant value for ca. 50 h, flow rate of 0.1 L/min)
V_{CO2} = 5 ppm (0.1 L/min)(3000 min) = 1.5 mL
T = 323 K
*N_{CO2} = PV/RT = (1 atm)(0.0015 L)/[(0.08206 atm*L/K*mol)(323K)] = 5.6x10^{-5} mol*
Current: I = ZNF/t = 2(5.6x10^{-5} mol) (96485 C/mol)/(1.8x10^5 s) = 6.1x10^{-5} A*
Area= 5 cm^2; J = 300 mA/cm^2
%Current(Carbonate removal) =100 6.1x10^{-5}A/(5*0.3 A) = 0.004%*

This Work: (Assume 5 ppm CO_2 being constantly generated)
Flow rate of 0.2 L/min; V_{CO2} = 5 ppm (0.2 L/min)(960 min) = 0.96 mL
T= 298 K
*N_{CO2} = (1 atm)(0.00096 L)/[(0.08206 atm*L/K*mol)(298K)] = 3.9x10^{-5} mol*
Current: (Z = 4 for this process) I = 4(3.9x10^{-5} mol)(96485 C/mol)/57600 s = 0.26 mA*
*%Current(Carbonate removal) = 100 * 0.26 mA / [(1.6 cm^2)(10 mA/cm^2)] = 1.7%*

References

(1) Bockris, J. O. Kinetics of Activation Controlled Consecutive Electrochemical Reactions: Anodic Evolution of Oxygen. *J. Chem. Phys.* **1956**, *24* (4), 817–827. https://doi.org/10.1063/1.1742616.

(2) Shinagawa, T.; Garcia-Esparza, A. T.; Takanabe, K. Insight on Tafel Slopes from a Microkinetic Analysis of Aqueous Electrocatalysis for Energy Conversion. *Sci. Rep.* **2015**, *5*, 1–21. https://doi.org/10.1038/srep13801.

(3) Watanabe, S.; Fukuta, K.; Yanagi, H. Determination of Carbonate Ion in MEA during Alkaline Membrane Fuel Cell (AMFC) Operation. *ECS Trans.* **2010**, *33* (1), 1837–1845.